Received: 12 August 2021 | Revised: 2 March 2022 | Accepted: 2 March 2022 | Published on: 1 April 2022
DOI: 10.1002/joc.7599

RESEARCH ARTICLE

International Journal of Climatology RMetS

Climatology of aerosol types and their vertical distribution over East Asia based on CALIPSO lidar measurements

Lu Gui[1,2] | **Minghui Tao**[1,2] | **Yi Wang**[1] | **Lunche Wang**[1,2] | **Liangfu Chen**[3] | **Changqing Lin**[4] | **Jinhua Tao**[3] | **Jun Wang**[5] | **Chao Yu**[3]

[1]Key Laboratory of Regional Ecology and Environmental Change, School of Geography and Information Engineering, China University of Geosciences, Wuhan, China

[2]Hubei Key Laboratory of Critical Zone Evolution, School of Geography and Information Engineering, China University of Geosciences, Wuhan, China

[3]State Key Laboratory of Remote Sensing Science, Aerospace Information Research Institute, Chinese Academy of Sciences, Beijing, China

[4]Institute for the Environment, Hong Kong University of Science & Technology, Hong Kong, China

[5]Center for Global and Regional Environmental Research, The University of Iowa, Iowa City, Iowa, USA

Correspondence

Minghui Tao, Key Laboratory of Regional Ecology and Environmental Change, School of Geography and Information Engineering, China University of Geosciences, No. 388, Lumo Road, Hongshan District, Wuhan 430074, China.
Email: taomh@cug.edu.cn

Funding information

National Natural Science Foundation of China, Grant/Award Numbers: 41830109, 41871262; Chinese Academy of Sciences

Abstract

Aerosol vertical distribution generally determines their health impacts and climate effects. By using long-term (2007–2019) CALIPSO lidar measurements, we present a large-scale insight into the climatology of aerosol types and their vertical structure over East Asia. Despite the low sampling frequency, comparison with MODIS aerosol optical depth (AOD) shows that the integrated CAIPSO vertical extinction can reasonably reproduce spatial patterns of the aerosol loading. With the unique advantage of active detection, CALIPSO reveals an obvious enhancement of the night-time AOD due to worse diffusion conditions. Moreover, long-range transport of different aerosols including dust, polluted dust, and smoke has substantial contribution to the aerosol loading over East Asia. Pure dust particles are mainly concentrated over the deserts with notable dust transport belts (dust AOD > 0.2 at 532 nm) along downwind regions during winter and spring. By contrast, polluted dust is prevalent over the downstream eastern China with much higher AODs throughout the year. In particular, AOD of polluted dust (~0.5) is higher in winter rather than in spring, which is consistent with their seasonal occurrences. Smoke aerosols usually appear in the night-time over southern China. The top heights of aerosols are around 4–6 km, with dust and smoke having higher extinction at upstream regions. The climatology of these aerosol types and vertical distribution can provide a significant constraint for associated studies of air quality and climate effects.

KEYWORDS

aerosol types, CALIPSO, occurrence frequency, vertical distribution

1 | INTRODUCTION

Tropospheric aerosols play a crucial role in the climate system by modifying Earth-atmosphere system's radiation budget and cloud properties (Kaufman *et al.*, 2002; Fan *et al.*, 2018; Christian *et al.*, 2019). Moreover, numerous epidemiological studies have shown robust correlations between the concentrations of these tiny particles and respiratory diseases (Pope III *et al.*, 2002). Besides aerosol loading, climate effects and health impacts of aerosols largely depend on their types and vertical distribution (Samset *et al.*, 2013; Mishra *et al.*, 2015; Seinfeld *et al.*, 2016). However, aerosol loading and properties have a very large spatial–temporal variability due to their short lifetime and diverse sources, exerting a great challenge in quantify their climate and health effects.

During the last decades, the advent of dedicated satellite instruments such as Moderate Resolution Imaging Spectroradiometer (MODIS), Multi-angle Imaging Spectroradiometer (MISR), and Polarization and Directionality of the Earth's Reflectance (POLDER) has greatly renewed the knowledge of global aerosol loading and major sources (Kaufman *et al.*, 2002). Although multi-angle and polarized measurements enables the retrievals of aerosol optical and microphysical properties, notable uncertainties exist due to deficiencies in algorithm assumptions and forward models (Dubovik *et al.*, 2019; Tao *et al.*, 2019; 2020a). By now, the most widely used satellite aerosol parameter is still MODIS aerosol optical depth (AOD). Compared with aerosol retrievals by passives instruments that have to separate surface contribution, Cloud-Aerosol Lidar with Orthogonal Polarization (CALIOP) sensor onboard the Cloud-Aerosol Lidar and Infrared Pathfinder Satellite Observation (CALIPSO) satellite has a striking advantage in discriminating typical aerosol types and their vertical distribution in both daytime and night-time (Hunt *et al.*, 2009; Winker *et al.*, 2009).

As one of the most polluted regions of the world, aerosols over East Asia are characterized by complicated mixtures of anthropogenic emissions, biomass burning fire smoke, and natural dust with large spatial and temporal variations (Li *et al.*, 2011; Tao *et al.*, 2020a). There have been numerous works concerning the long-term variations of aerosol over East Asia with both passive MODIS AODs and active CALIPSO aerosol profiles (Guo *et al.*, 2016; Huang *et al.*, 2013; Liu *et al.*, 2008; 2019; Proestakis *et al.*, 2018; Tao *et al.*, 2020b). However, previous studies usually focus on aerosol loading or vertical profiles of airborne dust. The recent CALIPSO extinction retrievals and aerosol classification methods have been substantially improved (Kim *et al.*, 2018; Young *et al.*, 2018), providing unprecedented chance to enhance understanding of the contributions of different aerosol types and their vertical distribution, especially in the night-time.

In this paper, we present a comprehensive insight into the climatology of different aerosols and their vertical distribution over East Asia based on CALIPSO measurements during 2007–2019. Section 2 introduces CALIPSO aerosol algorithms and MODIS aerosol products used. The general performance of CALIPSO AOD is evaluated by intercomparison with MODIS retrievals in section 3.1. Then, the contribution of different aerosol types to the aerosol loading over East Asia and their occurrence frequency are examined. Moreover, vertical characteristics of these aerosol types are compared and analysed. Additionally, the uncertainties of CALIPSO aerosol classification and extinction are discussed. At last, conclusions are followed in section 4.

2 | DATA AND METHOD

2.1 | CALIPSO aerosol datasets

The CALIOP lidar aboard CALIPSO satellite launched in April 2006 measures the total attenuated backscatter of aerosols at 532 and 1,064 nm with an additional perpendicular polarization detection at 532 nm (Liu *et al.*, 2008). By a 16-day revisiting cycle, CALIOP can observe both daytime and night-time aerosol and cloud backscatter profiles from the sea level to ~30 km, with higher signal-noise-ratio in the night without the background solar noise (Getzewich *et al.*, 2018). Despite a finer resolution, the Level (L) 2 CALIPSO aerosol profile products are reported at a uniform horizontal resolution of 5 or 40 km as well as a vertical resolution within 60–360 m to account for weak backscatter signals from aerosols. With a prescribed aerosol extinction-to-backscatter (lidar ratio), CALIOP AOD of the columnar extinction can be calculated. Meanwhile, the attenuated backscatter and depolarization ratio measurements can be used to identify aerosol and cloud types based on location, altitudes, and surface types (Omar *et al.*, 2009; Kim *et al.*, 2018).

The recent Version (V) 4.1 CALIPSO aerosol products have been substantially improved in extinction and optical depth (Young *et al.*, 2018) and aerosol classification (Kim *et al.*, 2018). Tropospheric aerosols in V4.1 CALIPSO are classified into seven subtypes including clean marine, dust, polluted continental/smoke, clean continental, polluted dust, elevated smoke, and dusty

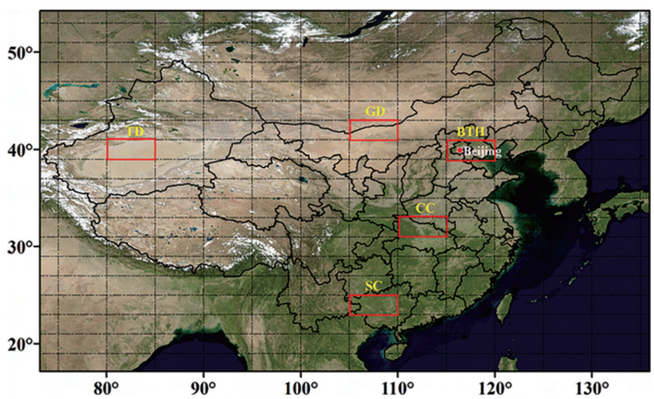

FIGURE 1 The terrain of mainland China (the black dashed lines indicate the grid of CALIOP L3 data, and the red boxes denote selected grids in Taklimakan Desert (TD), Gobi Desert (GD), Beijing–Tianjin–Hebei (BTH), central China (CC), and southern China (SC) [Colour figure can be viewed at wileyonlinelibrary.com]

marine. The L3 CALIPSO products provide global gridded, quality-screened, monthly mean profiles of aerosol extinction and subtypes at a uniform 2° × 5° grid (Tackett *et al.*, 2018). The total AOD of dust, polluted dust, and elevated smoke is also reported. CALIPSO AOD exhibits high consistency with collocated MODIS retrievals with relatively lower differences over East Asia (Young *et al.*, 2018). In this study, we utilize the L3 V4.1 CALIPSO cloud-free aerosol products in both daytime and night-time.

2.2 | MODIS aerosol optical depth

MODIS onboard the afternoon Aqua satellite since 2002 measures spectral irradiance of Earth-atmosphere system by 36 channels within 0.4–14 μm at nominal spatial resolutions of 250–1,000 m. With a wide swath width of ~2,330 km, MODIS can provide a near-daily global coverage. Unlike the active detection of CALIOP, MODIS aerosol retrievals have to separate the surface contribution by assumed spectral relationship or precalculated database of the surface reflectance (Hsu *et al.*, 2013). Ground-based validations show that MODIS deep blue (DB) aerosol algorithm has a robust performance in high-AOD conditions of East Asia (Tao *et al.*, 2019; Wei *et al.*, 2019). Thus, we select the C6.1 MODIS 10km DB AOD with good quality at 550 nm to make an intercomparison with CALIPSO results.

2.3 | Background of the study region

As shown in Figure 1, extensive deserts including Taklamakan Desert (TD) and the Gobi deserts (GD) exist

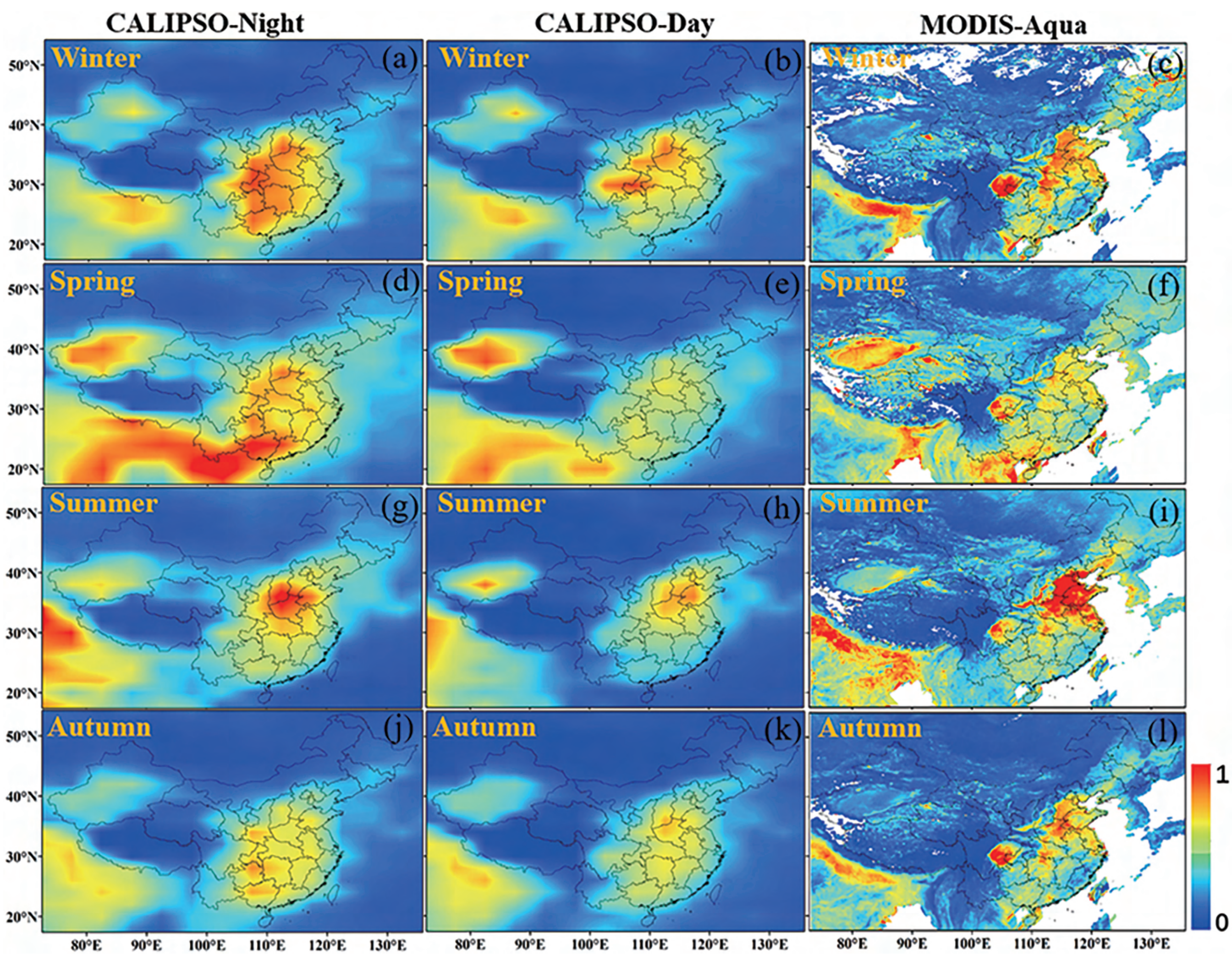

FIGURE 2 Seasonal AOD at 532 nm over East Asia from CALIPSO-Night (left column), CALIPSO-Day (middle column), and MODIS-Aqua (right column) [Colour figure can be viewed at wileyonlinelibrary.com]

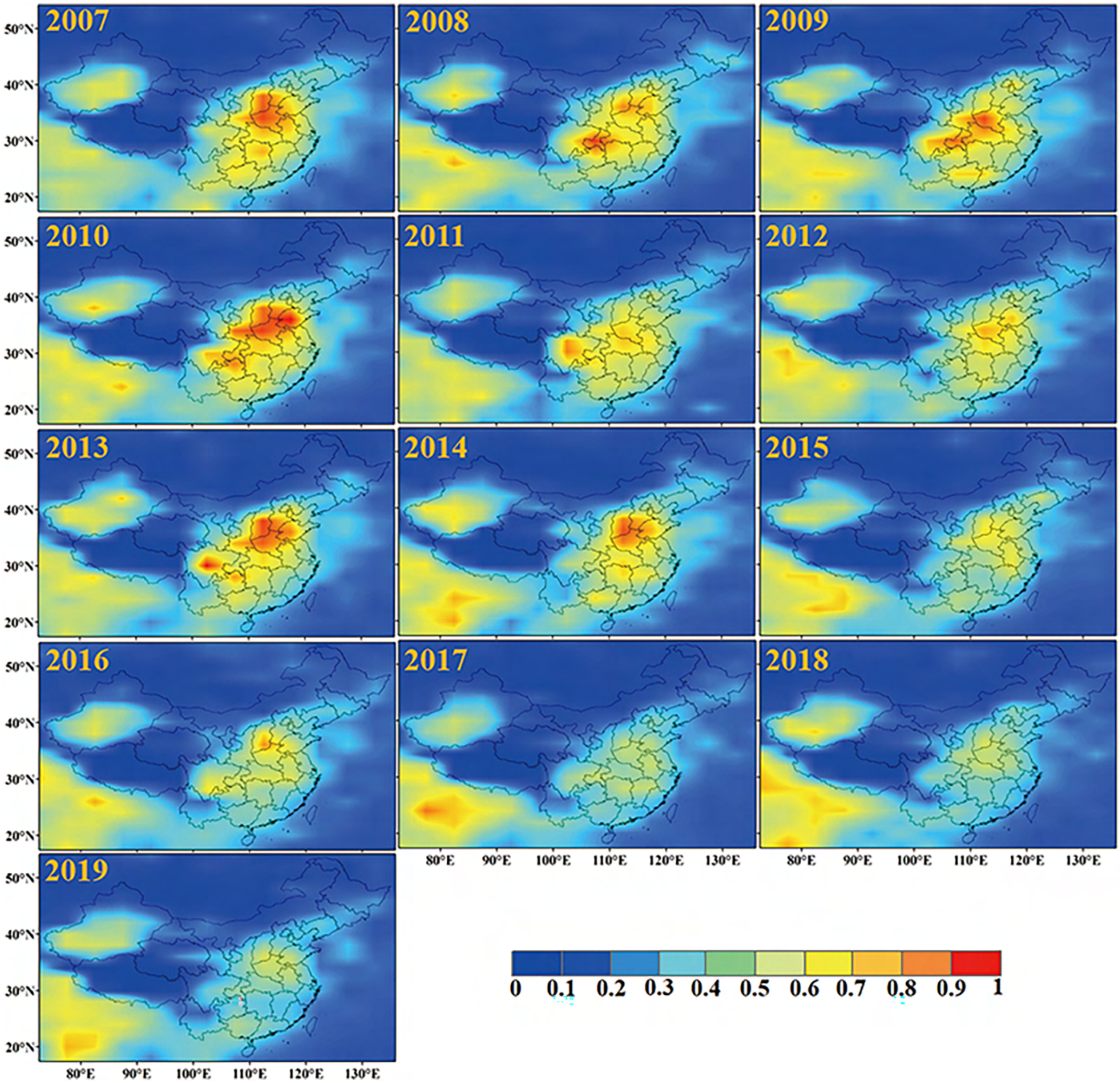

FIGURE 3 CALIPSO daytime AOD at 532 nm during 2007–2019 over East Asia [Colour figure can be viewed at wileyonlinelibrary.com]

in the northwestern part of East Asia. Most population and urban/industrial emissions are concentrated in northern China. By contrast, the terrain of southern China is by mountains and hills with much lower aerosol loading (Tao *et al*., 2020a). Five CALIPSO L3 grids in TD, GD, Beijing-Tianjin-Hebei (BTH), central China (CC), and southern China (SC) are selected to examine vertical extinction of aerosols. The CALIPSO $2^\circ \times 5^\circ$ grid is downscaled to $0.1^\circ \times 0.1^\circ$ by bilinear interpolation and smoothed.

3 | RESULTS AND DISCUSSIONS

3.1 | Climatology of CALIPSO AOD and intercomparison with MODIS products

Figure 2 shows seasonal AOD maps during 2007–2019 from MODIS at 550 nm and daytime and night-time CALIPSO products at 532 nm. The daytime CALIPSO AOD exhibits consistent spatial patterns with MODIS results for all seasons. Compared with MODIS AOD,

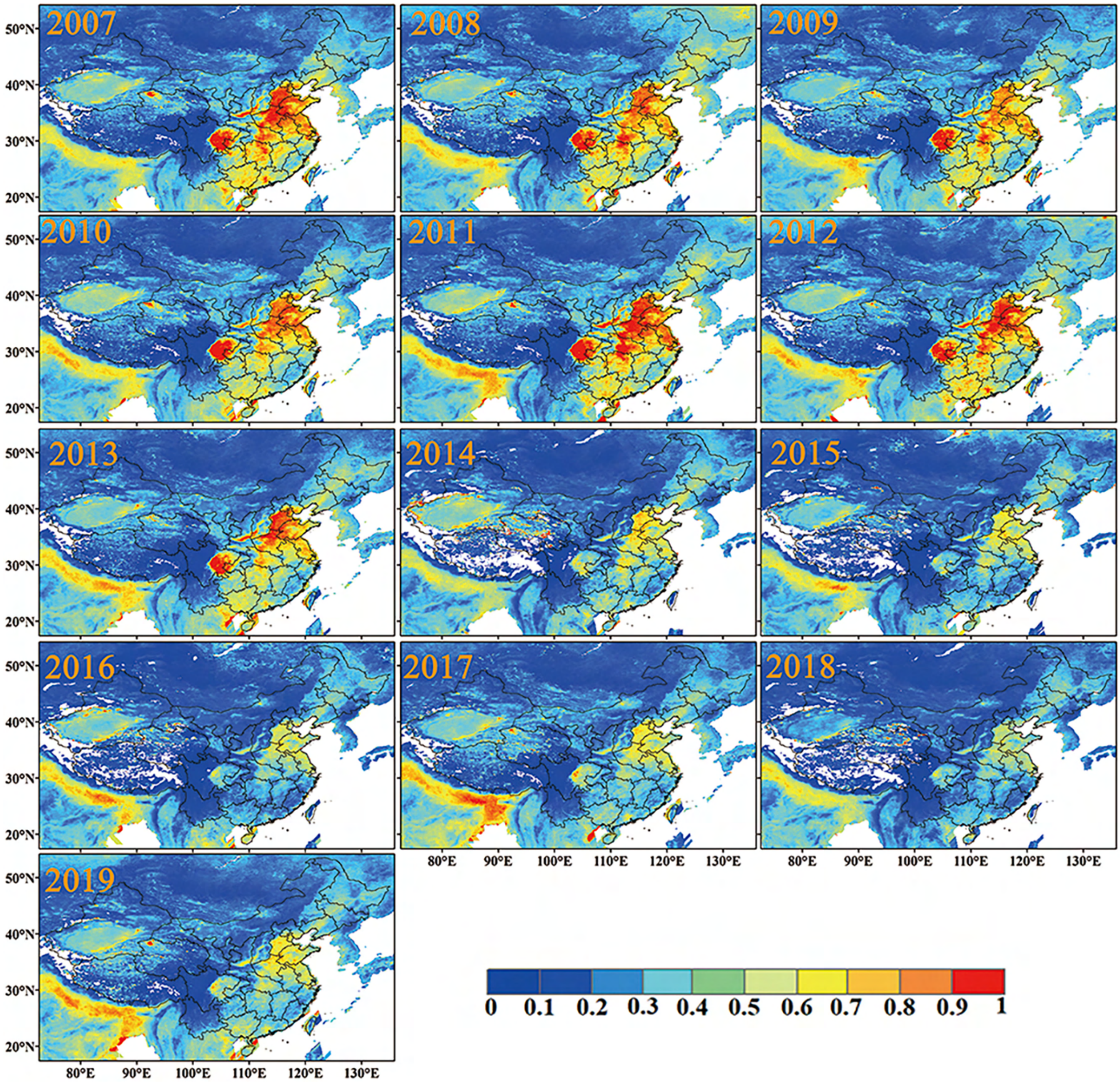

FIGURE 4 MODIS DB AOD at 550 nm during 2007–2019 over East Asia [Colour figure can be viewed at wileyonlinelibrary.com]

CALIPSO retrievals tend to overestimate aerosol loadings over the deserts and underestimate those in polluted regions such as northern China. Sampling frequency of satellite AOD has considerable influence on their seasonal or annual mean values in regions with high daily variations of aerosol loading (Tao *et al*., 2020b). Also, fixed lidar ratios of the aerosol subtypes in CALIPSO retrievals can introduce systematic bias in the extinction estimation (Amiridis *et al*., 2013; Young *et al*., 2018). Even with a low sampling frequency, CALIPSO retrievals have a better coverage and more reasonable performance than MODIS ones in some special regions such as northern Mongolia with bright snow/ice surfaces or Tibetan Plateau with very low aerosol loadings. In general, long-term mean of CALIPSO AOD can well capture spatial patterns of the aerosol loading over East Asia.

The active detection of CALIPSO products gives a unique view in spatial patterns of aerosol loading over East Asia in the night-time (Figure 2). While aerosol loading exhibits only slight changes over the deserts, CALIPSO AOD in eastern China is obviously enhanced during the night due largely to the much weaker convection and diffusion at lower temperatures (Tao *et al*., 2021). In particular, there is a notable aerosol

International Journal of Climatology RMetS

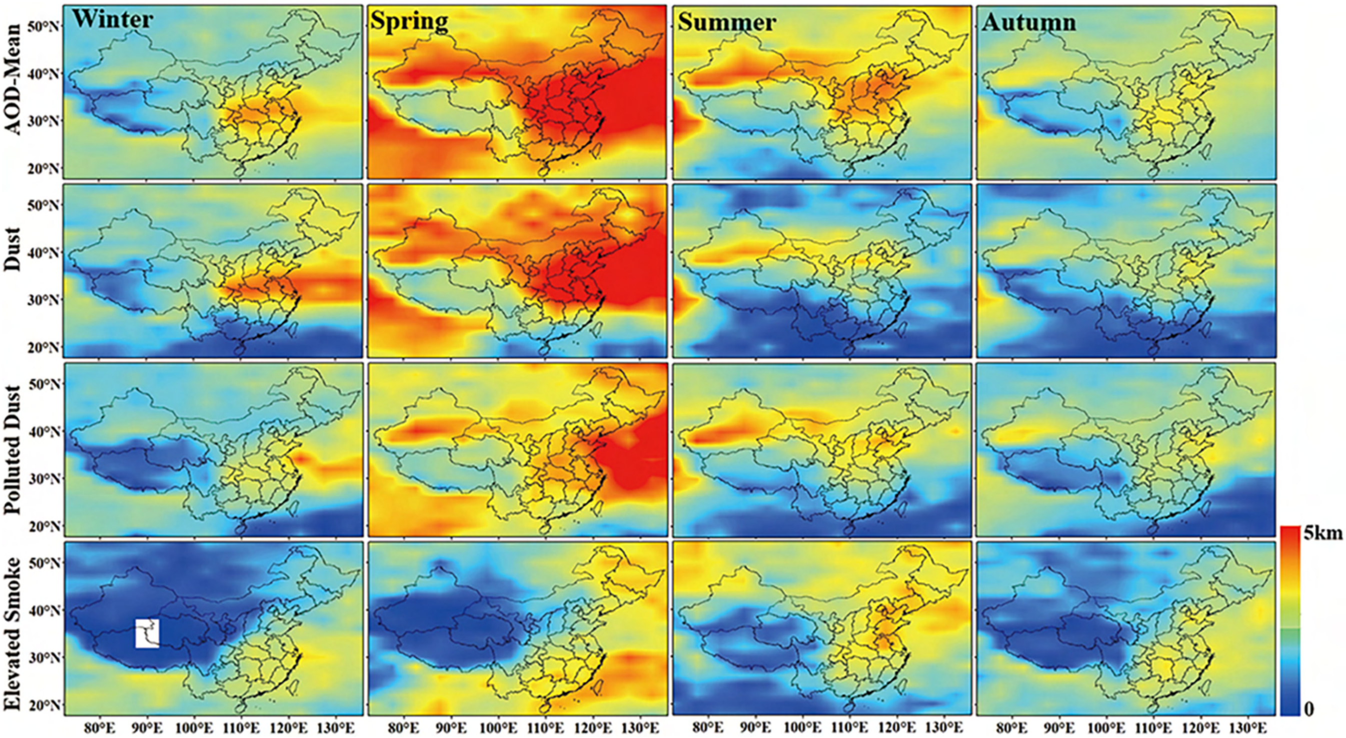

FIGURE 5 Seasonal distribution of top heights of the aerosol layers over East Asia from CALIPSO night-time products [Colour figure can be viewed at wileyonlinelibrary.com]

transport belt from Southeast Asia to southwestern China during spring, the AOD of which gets much larger than that in the daytime. The prevailing southwestern airmasses can transport emission of the intense biomass burning in spring downstream (Figure S1, Supporting Information) (Tsay *et al*., 2013). Also, the diurnal cycles of biomass burning in Southeast Asia can be an important factor. The CALIPSO AOD hotspots spread from northern China to southern China in the night-time, indicating the existence of regularly inter-regional transport (Tao *et al*., 2014). By contrast, close values of day and night CALIPSO AOD values over the deserts and background regions demonstrate that other factors such as assumed lidar ratio and higher night-time signal-noise ratio have no significant influences on their differences.

Figure 3 displays the temporal variations of annual daytime CALIPSO AOD during 2007–2019 over East Asia. Consistent with long-term variations of MODIS AOD (Tao *et al*., 2020b), CALIPSO can well reflect the declining aerosol loading in eastern China since 2013 due to the clean air actions of the government (Figure S2). However, spatial patterns of CALIPSO and MODIS AODs have substantial discrepancy in detailed scales (Figure 4). In particular, CALIPSO AOD cannot show spatial variations of the striking emission hotspots at finer spatial scales. For a timescale of annual mean, CALIPSO with a low sampling frequency can only capture limited information of the diverse pollution events. Annual variations of night-time CALIPSO AOD have similar trends but with higher values (Figure S3).

Despite the insufficient spatial and temporal resolutions in characterizing short-term spatial variations of aerosol loading, CALIPSO vertical detection of aerosol optical properties can provide valuable information concerning aerosol types and transport. To inspect the potential of aerosol transport over East Asia, seasonal variations of the night-time top heights of different aerosol types are shown in Figure 5. The aerosol plumes exhibit largest transport potential during spring with top heights around 5 km over both the deserts in the northwestern part and biomass burning regions of Southeast Asia even in the night (Tsay *et al*., 2013; An *et al*., 2018). The top heights of aerosols in other seasons decrease to 3–4 km, and get lower obviously as the distance from the emission sources increases. Moreover, top heights of different aerosol types have distinct differences in the spatial patterns and magnitudes.

3.2 | Contribution and occurrence frequency of different aerosol types

To examine the contribution of different aerosol types in East Asia, night-time CALIPSO AOD of typical

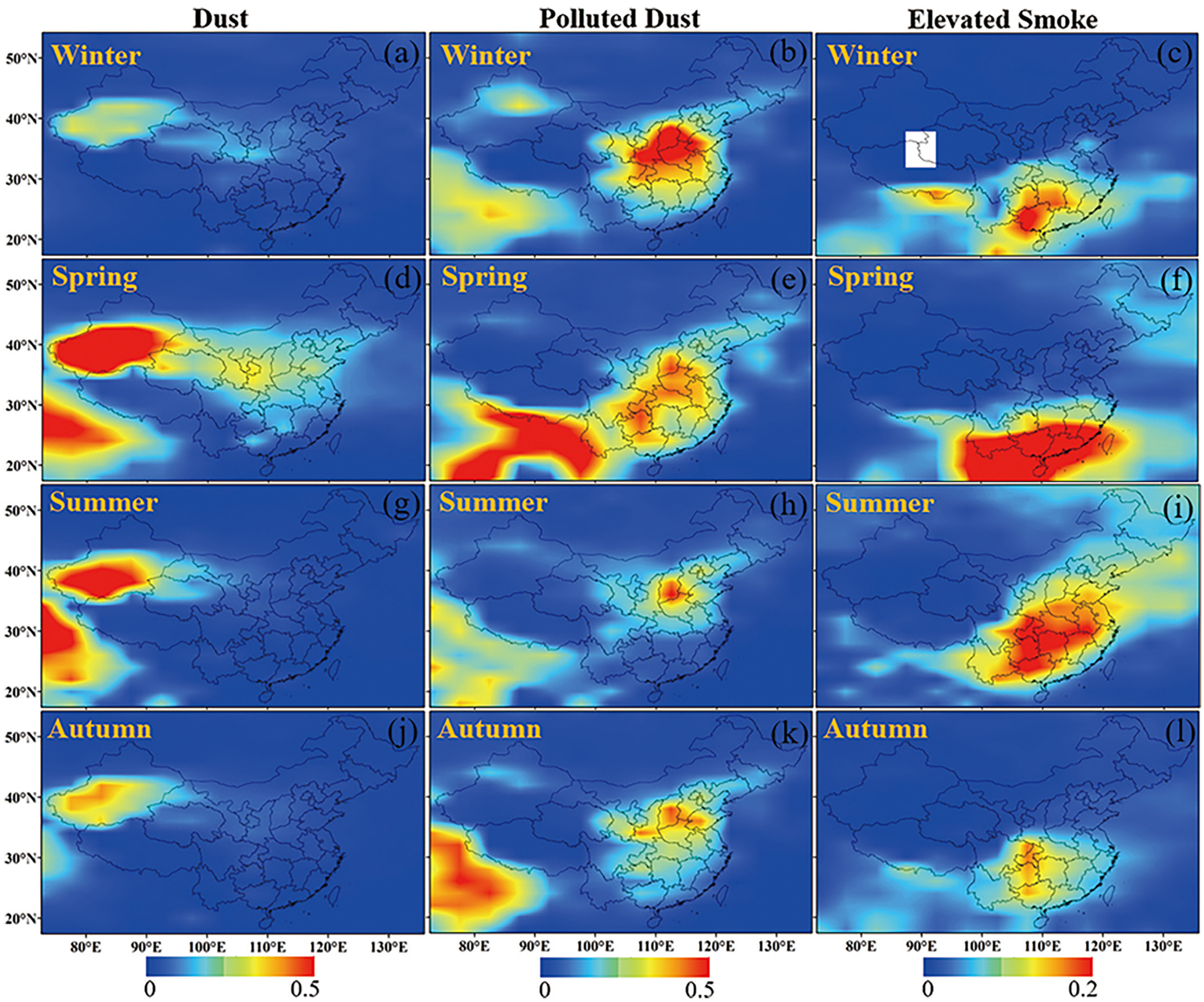

FIGURE 6 Seasonal distribution of CALIPSO night-time AOD at 532 nm of different aerosol types over East Asia [Colour figure can be viewed at wileyonlinelibrary.com]

aerosol types including dust, polluted dust, and elevated smoke are shown in Figure 6. Long-range transport of airborne dust has a substantial contribution to the aerosol loading over East Asia (Figure S4). While pure dust particles are predominated in the deserts and their transport path in the northwest, AOD of polluted dust (~0.5) in eastern China is much higher than that of the pure dust (~0.2–0.3). Unlike the pure dust that is most abundant in spring, AOD of polluted dust in highest during winter, which can be associated with the favourable meteorological conditions for dust-pollution mixing (Tao *et al.*, 2021). By contrast, elevated smoke is concentrated over southern China with highest AOD (>0.2) in spring. The frequency distribution plots of AOD in different areas during daytime and night-time are consistent with the spatial distribution trends of AOD values for different aerosol types (Figures S5 and S6).

Compared with CALIPSO AOD of dust particles in the night-time, pure dust exhibits no obvious changes in the AODs during the daytime (Figure 7). Although the heights of planetary boundary layer (PBL) are usually much higher in the daytime with notable convection, the AOD values of polluted dust get lower obviously in spring and summer, which can be partly caused by the lower levels of anthropogenic pollution (Figure 2). The CALIPSO algorithm classifies aerosol layers with a top height >2.5 km and low depolarization ratio as elevated smoke (Kim *et al.*, 2018). However, AODs values of the prevailing smoke over southern China in the night become much lower in the daytime during all the seasons, which seems contradictory with the favourable

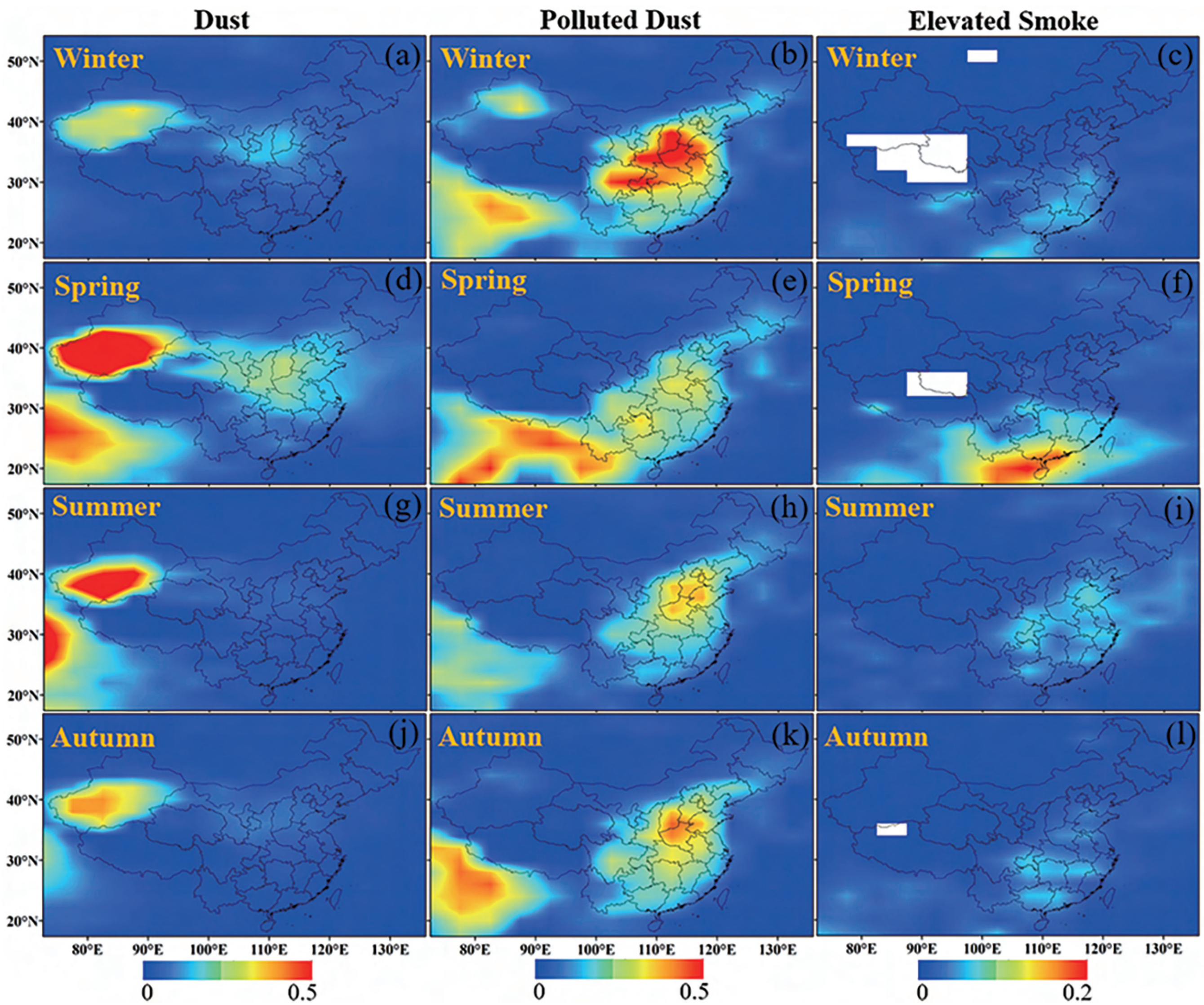

FIGURE 7 Seasonal distribution of CALIPSO daytime AOD at 532 nm of different aerosol types over East Asia [Colour figure can be viewed at wileyonlinelibrary.com]

meteorological conditions. Considering that the smoke layers from intense biomass burning fires can be easily injected to high altitudes of 3–5 km above the PBL (Tsay *et al.*, 2013), more night-time transport of fire smoke can be the main cause.

Furthermore, occurrence frequency of CALIPSO aerosol subtypes at different altitudes are calculated in Figure 8. Dust particles over the TD are lifted to high altitudes of 4–10 km during spring, and most dust layers tend to drop to 2–4 km in the transport path to eastern China. By contrast, occurrence frequency of dust particles above 6 km is much lower over TD during winter and autumn, with top heights of most dust layers at 4–6 km. However, the prevalent occurrence of polluted dust above 4–6 km indicates that considerable fraction of the pure dust with moderate depolarization ratio can be classified as polluted dust. Distribution of elevated smoke is mostly below 4 km in southern China and can reach 6 km in northeastern China. Some high occurrences of smoke appear at 8–10 km over the northern part except in winter, which can be caused by strong forest fires and misclassification of the dust aerosols (Liao et al., 2021). The polluted continental and dusty marine aerosols are usually within 2 km near surface. In addition, the clean marine aerosols are concentrated below 1 km.

CALIPSO vertical detection shows prevailing transport of natural dust and fire smoke over East Asia. These long-range transports usually occur above PBL, and their mixing with local anthropogenic emissions can be further delayed due to common temperature inversions in eastern China (Tao *et al.*, 2021). It is worth

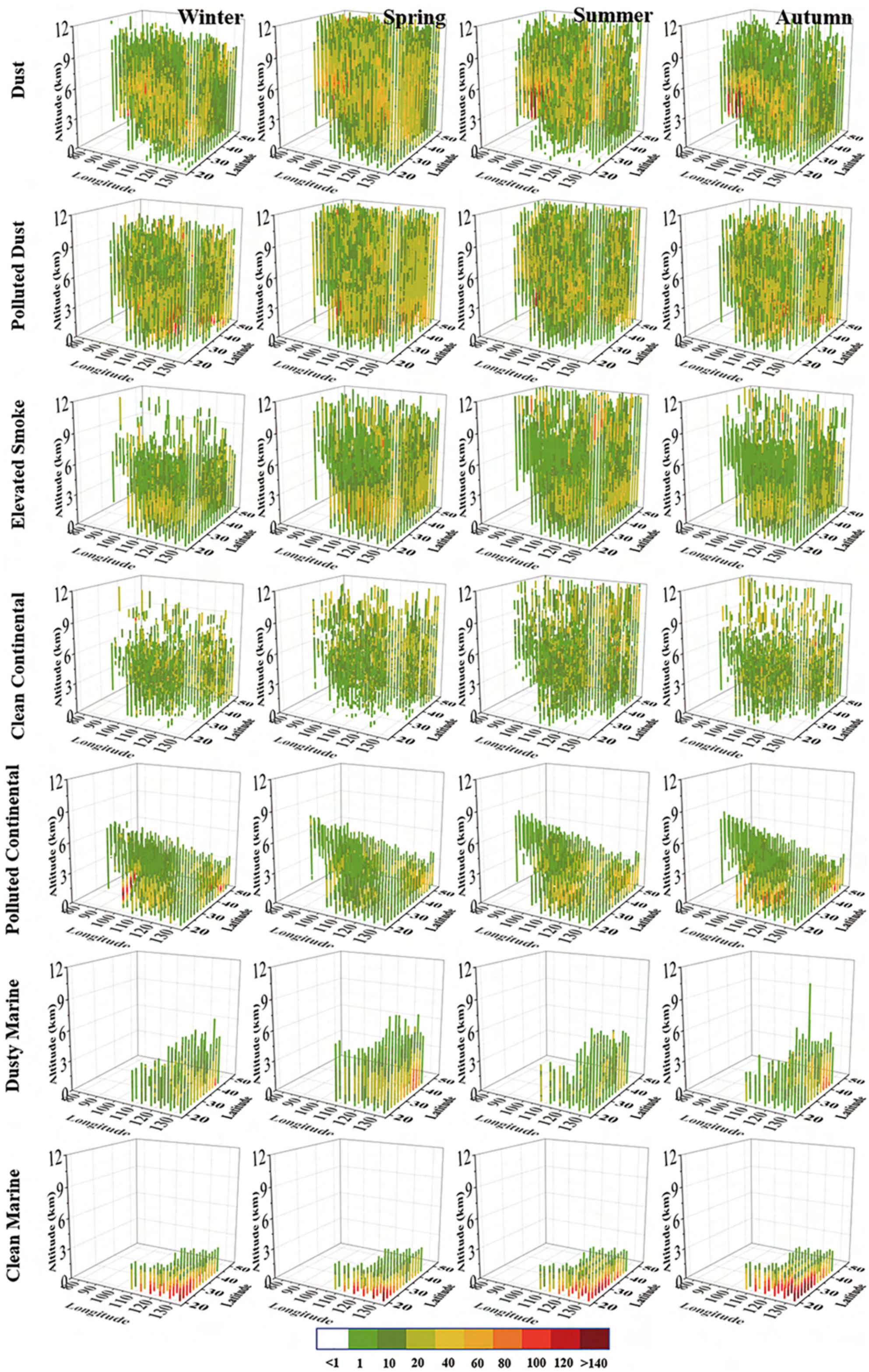

FIGURE 8 Seasonal occurrence frequency of night-time CALIPSO aerosol subtypes in East Asia during 2007–2019 [Colour figure can be viewed at wileyonlinelibrary.com]

noting that mean values of the top heights for dust and smoke layers in the downstream regions such as eastern China are even higher than the sources (Figures 5 and 8), which can be lifted to higher altitudes in the transport. However, CALIPSO AOD gets much lower when aerosol transport arrives over the sea in the eastern part. While airborne dust tends to have the largest transport potential in spring, AOD of the elevated smoke over the sea is high (>0.1) during both spring and summer (Figure 6).

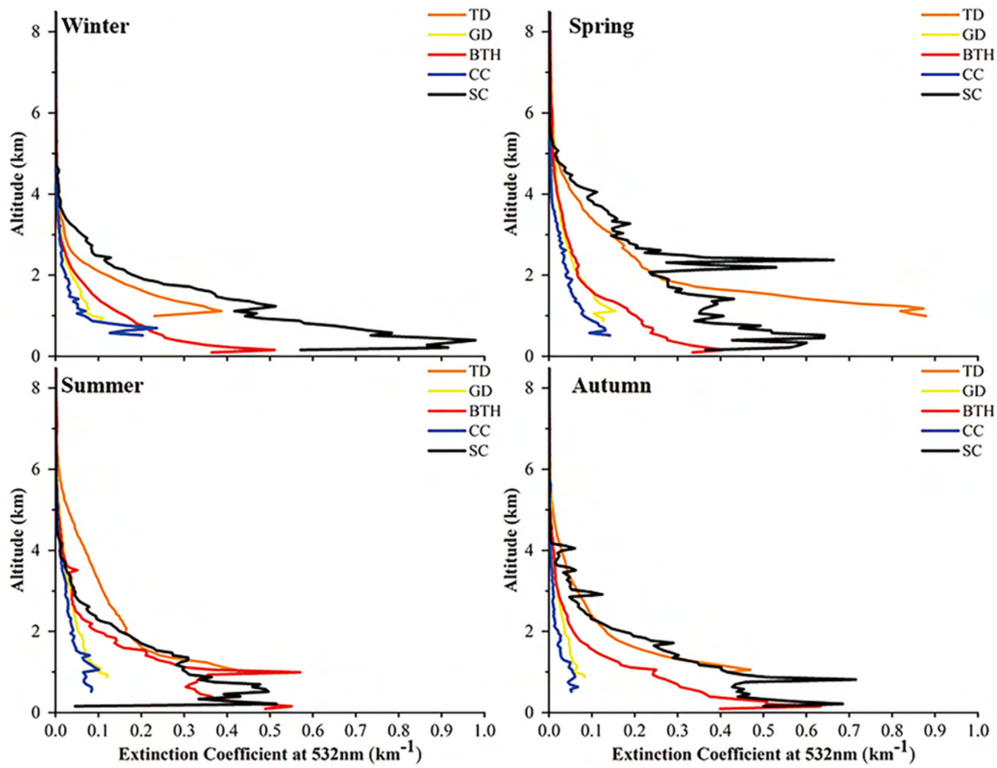

FIGURE 9 Seasonal night-time aerosol extinction coefficient profiles in Taklamakan Desert (TD), the Gobi deserts (GD), Beijing–Tianjin–Hebei (BTH), central China (CC), and southern China (SC) during 2007–2019 [Colour figure can be viewed at wileyonlinelibrary.com]

TABLE 1 Number of monthly CALIPSO night-time extinction profiles at 532 nm during 2007–2019

Winter	TD	37
	GD	38
	BTH	38
	CC	38
	SC	37
Spring	TD	39
	GD	39
	BTH	39
	CC	39
	SC	38
Summer	TD	39
	GD	39
	BTH	39
	CC	39
	SC	32
Fall	TD	39
	GD	39
	BTH	39
	CC	39
	SC	39

3.3 | CALIPSO extinction coefficient profiles of different aerosol types

To explore vertical variations of the aerosol loading, seasonal extinction profiles of different aerosol types are compared in typical regions of East Asia (Figure 9). The night-time extinction coefficients of airborne dust over the TD are about 2–3 times or even more of those in the downstream BTH and CC. It is surprising that the extinction coefficients above 2 km in SC are higher than those over TD in winter and spring with notable peaks above surface pollution layers (Figures 2 and 3). On the other hand, extinction coefficients near surface in SC are much higher than in BTH. Since anthropogenic emissions are mostly concentrated in northern China (Tao *et al.*, 2020a), the extreme high values (~0.6–1.0) of extinction coefficients in SC during should be paid to more attention. Considering the CALIPSO results used are seasonal mean values of during 2007–2019, with the low sampling frequency (Table 1), extinction profiles of the numerous aerosol transport events with distinct vertical variations can be largely smoothed.

Figure 10 gives seasonal extinction profiles of dust, polluted dust, and elevated smoke. Although occurrence frequency shows prevalent airborne dust in the high

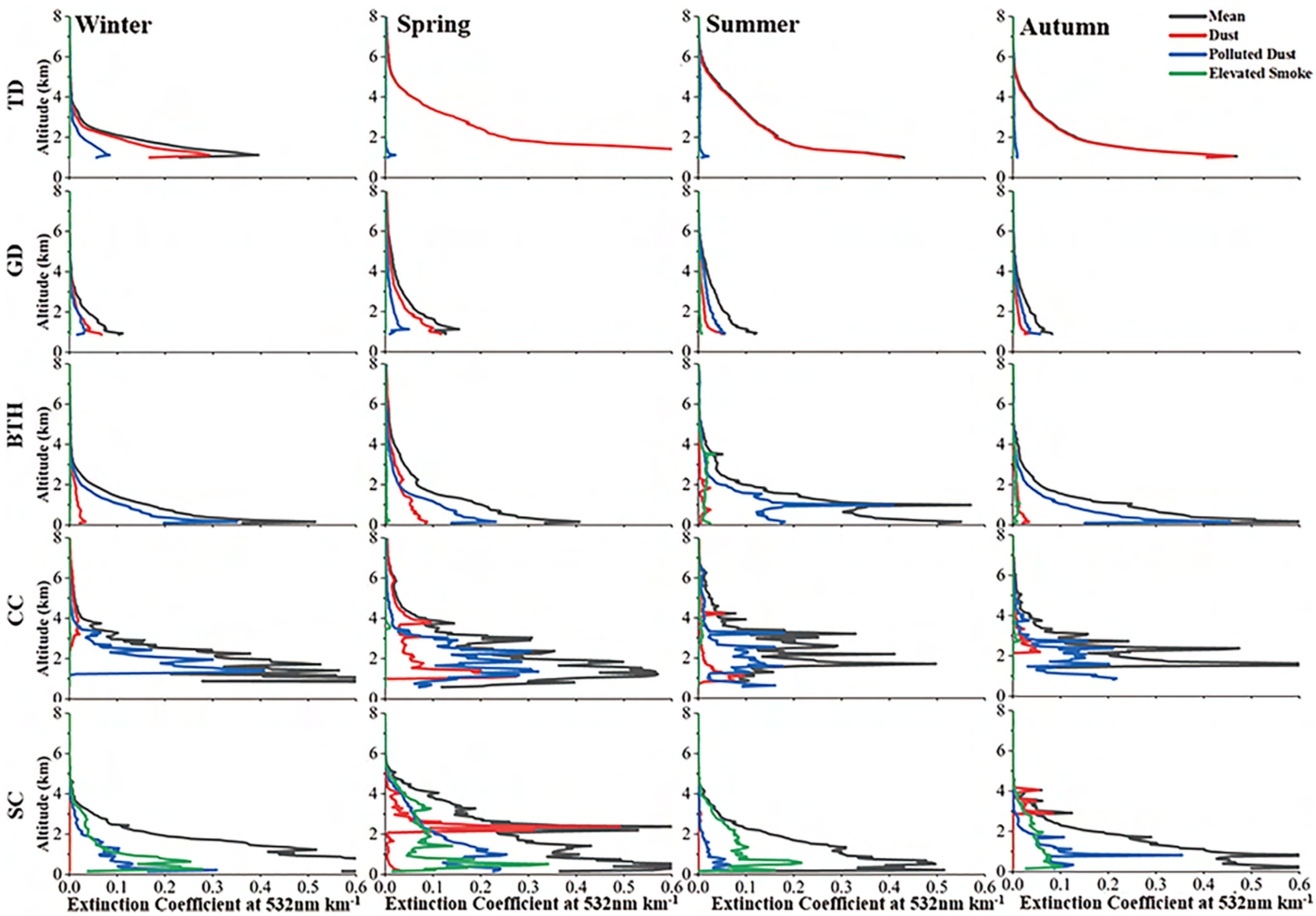

FIGURE 10 Seasonal night-time extinction coefficient of the total aerosols (mean), dust, polluted dust, and elevated smoke in TD, GD, BTH, CC, and SC during 2007–2019 [Colour figure can be viewed at wileyonlinelibrary.com]

altitudes of 6–10 km, CALIPSO extinction profiles demonstrate that these dust particles above 6 km usually have very low concentration except the few dust storms. While pure dust is predominant in the aerosols over deserts, polluted dust accounts for a much larger contribution in BTH and CC, which is consistent with prevalent dust transport in eastern China (Tao *et al*., 2022). The mean extinction values of polluted dust are very close to those of the total aerosols. Striking peak values (~0.3) of polluted dust appear over CC rather than in BTH of northern China, which can be due to that dust events in CC with lower frequency can be less influenced by the seasonal mean smooth. Seasonal mean values of extinction coefficients from the elevated smoke are very low (<0.1) except in SC.

Generally, the long-term CALIPSO measurements provide a fundamental knowledge concerning vertical distribution of typical aerosols including airborne dust and fire smoke over East Asia. Although previous studies usually focus on anthropogenic pollution near surface, prevalent transport of the elevated dust and smoke aerosols can play a significant role in regional atmospheric environment and climate change. Also, diurnal cycles such as night-time enhancement of the elevated smoke should be further examined with more observations such as ground-based lidar. In particular, the contribution of these substantial aerosol transport as well as their influence on local atmospheric chemistry and aerosol climate effects remain unclear. It should be stated that notable uncertainties exist in CALIPSO aerosol classification such as dust and polluted dust (Kim *et al*., 2018; Song *et al*., 2021). Considering the unique advantage of CALIPSO detection, the improvements on CALIPSO algorithm based on aerosol properties such as lidar ratio and depolarization ratios of different dust particles over East Asia are in need.

4 | CONCLUSIONS

The advent of dedicated satellite instruments has greatly renewed the knowledge of global aerosol loading.

However, further application of satellite products in studies of air quality and climate effects has been hindered due to the lack of sufficient aerosol information such as aerosol types and vertical distribution. CALIPSO lidar measurements can not only detect vertical characteristics of aerosol properties, but also give a unique view of the night-time aerosols with the active detection. In this study, based on the long-term CALIPSO monthly data during 2007–2019, we analysed the climatology of typical aerosol types including dust, polluted dust, and smoke as well as their vertical distribution in both daytime and night-time over East Asia.

Despite a low sampling frequency, CALIPSO daytime columnar AOD exhibits reasonable consistency with MODIS products. With the advantage of discriminating different aerosol types, CALIPSO detection shows that long-range transport of dust, polluted dust, and smoke has a large contribution to the aerosol loading over East Asia. While pure dust particles are concentrated over the Taklimakan Desert with notable dust belt along the downstream transport path, polluted dust is prevalent in eastern China. Moreover, polluted dust particles are most abundant and frequent during winter rather than spring with high dust AODs around ~0.5, due most likely to favourable meteorological conditions for dust-pollution mixing. By contrast, smoke aerosols usually appear in the night over southern China. The top heights of dust and smoke aerosols are around 4–6 km with much higher loading above the PBL than these in downstream regions. The valuable information of CALIPSO measurements can significantly fill the gap of global aerosol properties. Additionally, more attention should be paid to validation and algorithm improvements of the CALIPSO products.

ACKNOWLEDGEMENTS

This study was supported by National Natural Science Foundation of China (Grant Nos. 41871262 and 41830109) and Strategic Priority Research Program of the Chinese Academy of Sciences (Grant No. XDA19040201). Jun Wang's participation is made possible via the in-kind support from the University of Iowa. We thank the CALIPSO and MODIS team for the data used in our work.

AUTHOR CONTRIBUTIONS

Lu Gui: Investigation; visualization; writing – original draft. **Minghui Tao:** Conceptualization; writing – review and editing. **Yi Wang:** Data curation; formal analysis. **Lunche Wang:** Formal analysis. **Liangfu Chen:** Project administration; resources; supervision. **Changqing Lin:** Formal analysis; resources. **Jinhua Tao:** Data curation; formal analysis. **Jun Wang:** Conceptualization. **Chao Yu:** Validation.

ORCID

Minghui Tao https://orcid.org/0000-0003-1472-2955

REFERENCES

Amiridis, V., Wandinger, U., Marinou, E., Giannakaki, E., Tsekeri, A., Basart, S., Kazadzis, S., Gkikas, A., Taylor, M., Baldasano, J. and Ansmann, A. (2013) Optimizing CALIPSO saharan dust retrievals. *Atmospheric Chemistry and Physics*, 13(23), 12089–12106.

An, L., Che, H., Xue, M., Zhang, T., Wang, H., Wang, Y., Zhou, C., Zhao, H., Gui, K., Zheng, Y., Sun, T., Liang, Y., Sun, E., Zhang, H. and Zhang, X. (2018) Temporal and spatial variations in sand and dust storm events in East Asia from 2007 to 2016: relationships with surface conditions and climate change. *Science of the Total Environment*, 633, 452–462.

Christian, K., Wang, J., Ge, C., Peterson, D., Hyer, E., Yorks, J. and McGill, M. (2019) Radiative forcing and stratospheric warming of pyrocumulonimbus smoke aerosols: first modeling results with multisensor (EPIC, CALIPSO, and CATS) views from space. *Geophysical Research Letters*, 46, 10061–10071.

Dubovik, O., Li, Z., Mishchenko, M.I., Tanré, D., Karol, Y., Bojkov, B., Cairns, B., Diner, D.J., Espinosa, W.R., Goloub, P., Gu, X., Hasekamp, O., Hong, J., Hou, W., Knobelspiesse, K.D., Landgraf, J., Li, L., Litvinov, P., Liu, Y., Lopatin, A., Marbach, T., Maring, H., Martins, V., Meijer, Y., Milinevsky, G., Mukai, S., Parol, F., Qiao, Y., Remer, L., Rietjens, J., Sano, I., Stammes, P., Stamnes, S., Sun, X., Tabary, P., Travis, L.D., Waquet, F., Xu, F., Yan, C. and Yin, D. (2019) Polarimetric remote sensing of atmospheric aerosols: instruments, methodologies, results, and perspectives. *Journal of Quantitative Spectroscopy and Radiative Transfer*, 224, 474–511.

Fan, J., Rosenfeld, D., Zhang, Y., Giangrande, S.E., Li, Z., Machado, L.A.T., Martin, S.T., Yang, Y., Wang, J., Artaxo, P., Barbosa, H.M.J., Braga, R.C., Comstock, J.M., Feng, Z., Gao, W., Gomes, H.B., Mei, F., Pöhlker, C., Pöhlker, M.L., Pöschl, U. and de Souza, R.A.F. (2018) Substantial convection and precipitation enhancements by ultrafine aerosol particles. *Science (New York, N.Y.)*, 359, 411–418.

Getzewich, B.J., Vaughan, M.A., Hunt, W.H., Avery, M.A., Powell, K.A., Tackett, J.L., Winker, D.M., Kar, J., Lee, K.-P. and Toth, T.D. (2018) CALIPSO lidar calibration at 532 nm: version 4 daytime algorithm. *Atmospheric Measurement Techniques*, 11, 6309–6326.

Guo, J., Liu, H., Wang, F., Huang, J., Xia, F., Lou, M., Wu, Y., Jiang, J. H., Xie, T., Zhaxi, Y. and Yung, Y.L. (2016) Three-dimensional structure of aerosol in China: a perspective from multi-satellite observations. *Atmospheric Research*, 178–179, 580–589.

Hsu, N.C., Jeong, M.J., Bettenhausen, C., Sayer, A.M., Hansell, R., Seftor, C.S., Huang, J. and Tsay, S.C. (2013) Enhanced deep blue aerosol retrieval algorithm: the second generation. *Journal of Geophysical Research: Atmospheres*, 118(16), 9296–9315.

Huang, L., Jiang, J.H., Tackett, J.L., Su, H. and Fu, R. (2013) Seasonal and diurnal variations of aerosol extinction profile and type distribution from CALIPSO 5-year observations. *Journal of Geophysical Research: Atmospheres*, 118, 4572–4596.

Hunt, W.H., Winker, D.M., Vaughan, M.A., Powell, K.A., Lucker, P.L. and Weimer, C. (2009) CALIPSO Lidar description and performance assessment. *Journal of Atmospheric and Oceanic Technology*, 26(7), 1214–1228.

Kaufman, Y.J., Tanré, D. and Boucher, O. (2002) A satellite view of aerosols in the climate system. *Nature*, 419, 215–223.

Kim, M.H., Omar, A.H., Tackett, J.L., Vaughan, M.A., Winker, D. M., Trepte, C.R., Hu, Y., Liu, Z., Poole, L.R., Pitts, M.C., Kar, J. and Magill, B.E. (2018) The CALIPSO version 4 automated aerosol classification and lidar ratio selection algorithm. *Atmospheric Measurement Techniques*, 11, 6107–6135.

Li, Z., Li, C., Chen, H., Tsay, S.C., Holben, B., Huang, J., Li, B., Maring, H., Qian, Y., Shi, G., Xia, X., Yin, Y., Zheng, Y. and Zhuang, G. (2011) East Asian studies of tropospheric aerosols and their impact on regional climate (EAST-AIRC): an overview. *Journal of Geophysical Research: Atmospheres*, 116(D7), D00K34.

Liao, T., Gui, K., Li, Y., Wang, X. and Sun, Y. (2021) Seasonal distribution and vertical structure of different types of aerosols in southwest China observed from CALIOP. *Atmospheric Environment*, 246, 118145.

Liu, D., Zhao, T., Boiyo, R., Chen, S., Lu, Z., Wu, Y. and Zhao, Y. (2019) Vertical structures of dust aerosols over East Asia based on CALIPSO retrievals. *Remote Sensing*, 11(6), 701. https://doi.org/10.3390/rs11060701.

Liu, Z., Liu, D., Huang, J., Vaughan, M., Uno, I., Sugimoto, N., Kittaka, C., Trepte, C., Wang, Z., Hostetler, C. and Winker, D. (2008) Airborne dust distributions over the Tibetan Plateau and surrounding areas derived from the first year of CALIPSO lidar observations. *Atmospheric Chemistry and Physics*, 8(16), 5045–5060.

Mishra, A.K., Koren, I. and Rudich, Y. (2015) Effect of aerosol vertical distribution on aerosol-radiation interaction: a theoretical prospect. *Heliyon*, 1, e00036.

Omar, A.H., Winker, D.M., Vaughan, M.A., Hu, Y., Trepte, C.R., Ferrare, R.A., Lee, K.-P., Hostetler, C.A., Kittaka, C., Rogers, R. R., Kuehn, R.E. and Liu, Z. (2009) The CALIPSO automated aerosol classification and lidar ratio selection algorithm. *Journal of Atmospheric and Oceanic Technology*, 26(10), 1994–2014.

Pope, C.A., III, Burnett, R.T., Thun, M.J., Calle, E.E., Krewski, D., Ito, K. and Thurston, G.D. (2002) Lung cancer, cardiopulmonary mortality, and long-term exposure to fine particulate air pollution. *JAMA*, 287, 1132–1141.

Proestakis, E., Amiridis, V., Marinou, E., Georgoulias, A.K., Solomos, S., Kazadzis, S., Chimot, J., Che, H., Alexandri, G., Binietoglou, I., Daskalopoulou, V., Kourtidis, K.A., de Leeuw, G. and Ronald, J. (2018) Nine-year spatial and temporal evolution of desert dust aerosols over South and East Asia as revealed by CALIOP. *Atmospheric Chemistry and Physics*, 18, 1337–1362.

Samset, B.H., Myhre, G., Schulz, M., Balkanski, Y., Bauer, S., Berntsen, T.K., Bian, H., Bellouin, N., Diehl, T., Easter, R.C., Ghan, S.J., Iversen, T., Kinne, S., Kirkevåg, A., Lamarque, J.F., Lin, G., Liu, X., Penner, J.E., Seland, Ø., Skeie, R.B., Stier, P., Takemura, T., Tsigaridis, K. and Zhang, K. (2013) Black carbon vertical profiles strongly affect its radiative forcing uncertainty. *Atmospheric Chemistry and Physics*, 13, 2423–2434.

Seinfeld, J.H., Bretherton, C., Carslaw, K.S., Coe, H., DeMott, P.J., Dunlea, E.J., Feingold, G., Ghan, S., Guenther, A.B. and Kahn, R. (2016) Improving our fundamental understanding of the role of aerosol−cloud interactions in the climate system. *Proceedings of the National Academy of Sciences of the United States of America*, 113(21), 5781–5790.

Song, Q., Zhang, Z., Yu, H., Ginoux, P. and Shen, J. (2021) Global dust optical depth climatology derived from CALIOP and MODIS aerosol retrievals on decadal timescales: regional and interannual variability. *Atmospheric Chemistry and Physics*, 21, 13369–13395.

Tackett, J.L., Winker, D.M., Getzewich, B.J., Vaughan, M.A., Young, S.A. and Kar, J. (2018) CALIPSO lidar level 3 aerosol profile product: version 3 algorithm design. *Atmospheric Measurement Techniques*, 11, 4129–4152.

Tao, M., Chen, L., Wang, J., Wang, L., Wang, W., Lin, C., Gui, L., Wang, L., Yu, C. and Wang, Y. (2022) Characterization of dust activation and their prevailing transport over East Asia based on multi-satellite observations. *Atmospheric Research*, 265, 105886.

Tao, M., Gui, L., Li, R., Wang, L., Liang, S., Li, Q., Wang, L., Yu, C. and Chen, L. (2021) Tracking prevailing dust aerosol over the air pollution in central China with integrated satellite and ground observations. *Atmospheric Environment*, 253, 118369.

Tao, M., Li, R., Wang, L., Lan, F., Wang, Z., Tao, J., Che, H., Wang, L. and Chen, L. (2020b) A critical view of long-term AVHRR aerosol data record in China: retrieval frequency and heavy pollution. *Atmospheric Environment*, 223, 117246.

Tao, M., Wang, J., Li, R., Chen, L., Xu, X., Wang, L., Tao, J., Wang, Z. and Xiang, J. (2020a) Characterization of aerosol type over East Asia by 4.4 km MISR product: first insight and general performance. *Journal of Geophysical Research: Atmospheres*, 125, e2019JD031909.

Tao, M., Wang, J., Li, R., Wang, L., Wang, L., Wang, Z., Tao, J., Che, H. and Chen, L. (2019) Performance of MODIS high-resolution MAIAC aerosol algorithm in China: characterization and limitation. *Atmospheric Environment*, 213, 159–169.

Tsay, S.-C., Hsu, N.C., Lau, W.K.M., Li, C., Gabriel, P.M., Ji, Q., Holben, B.N., Judd Welton, E., Nguyen, A.X., Janjai, S., Lin, N. H., Reid, J.S., Boonjawat, J., Howell, S.G., Huebert, B.J., Fu, J. S., Hansell, R.A., Sayer, A.M., Gautam, R., Wang, S.H., Goodloe, C.S., Miko, L.R., Shu, P.K., Loftus, A.M., Huang, J., Kim, J.Y., Jeong, M.J. and Pantina, P. (2013) From BASE-ASIA toward 7-SEAS: a satellite-surface perspective of boreal spring biomass-burning aerosols and clouds in Southeast Asia. *Atmospheric Environment*, 78, 20–34.

Wei, J., Li, Z., Peng, Y. and Sun, L. (2019) MODIS collection 6.1 aerosol optical depth products over land and ocean: validation and comparison. *Atmospheric Environment*, 201, 428–440.

Winker, D.M., Vaughan, M.A., Omar, A., Hu, Y., Powell, K.A., Liu, Z., Hunt, W.H. and Young, S.A. (2009) Overview of the CALIPSO Mission and CALIOP data processing algorithms. *Journal of Atmospheric and Oceanic Technology*, 26(11), 2310–2323.

Young, S.A., Vaughan, M.A., Garnier, A., Tackett, J.L., Lambeth, J. D. and Powell, K.A. (2018) Extinction and optical depth retrievals for CALIPSO's version 4 data release. *Atmospheric Measurement Techniques*, 11, 5701–5727.

SUPPORTING INFORMATION

Additional supporting information may be found in the online version of the article at the publisher's website.

How to cite this article: Gui, L., Tao, M., Wang, Y., Wang, L., Chen, L., Lin, C., Tao, J., Wang, J., & Yu, C. (2022). Climatology of aerosol types and their vertical distribution over East Asia based on CALIPSO lidar measurements. *International Journal of Climatology*, *42*(11), 6042–6054. https://doi.org/10.1002/joc.7599